

Interpolatory methods for \mathcal{H}_∞ model reduction of multi-input/multi-output systems*

Alessandro Castagnotto, Christopher Beattie, and Serkan Gugercin

Abstract We develop here a computationally effective approach for producing high-quality \mathcal{H}_∞ -approximations to large scale linear dynamical systems having multiple inputs and multiple outputs (MIMO). We extend an approach for \mathcal{H}_∞ model reduction introduced by Flag, Beattie, and Gugercin [1] for the single-input/single-output (SISO) setting, which combined ideas originating in interpolatory \mathcal{H}_2 -optimal model reduction with complex Chebyshev approximation. Retaining this framework, our approach to the MIMO problem has its principal computational cost dominated by (sparse) linear solves, and so it can remain an effective strategy in many large-scale settings. We are able to avoid computationally demanding \mathcal{H}_∞ norm calculations that are normally required to monitor progress within each optimization cycle through the use of “data-driven” rational approximations that are built upon previously computed function samples. Numerical examples are included that illustrate our approach. We produce high fidelity reduced models having consistently better \mathcal{H}_∞ performance than models produced via balanced truncation; these models often are as good as (and occasionally better than) models produced using optimal Hankel norm approximation as well. In all cases considered, the method described here produces reduced models at far lower cost than is possible with either balanced truncation or optimal Hankel norm approximation.

Alessandro Castagnotto

Technical University of Munich, Garching bei München e-mail: a.castagnotto@tum.de

Christopher Beattie

Virginia Tech, Blacksburg, VA 24061 USA e-mail: beattie@vt.edu

Serkan Gugercin

Virginia Tech, Blacksburg, VA 24061 USA e-mail: gugercin@vt.edu

* The work of the first author was supported by the German Research Foundation (DFG), Grant LO408/19-1, as well as the TUM Fakultäts-Graduiertenzentrum Maschinenwesen; the work of the second author was supported by the Einstein Foundation - Berlin; the work of the third author was supported by the Alexander von Humboldt Foundation.

Accepted to appear in *Model Reduction of Parametrized Systems III*, Springer.

1 Introduction

The accurate modeling of dynamical systems often requires that a large number of differential equations describing the evolution of a large number of state variables be integrated over time to predict system behavior. The number of state variables and differential equations involved can be especially large and forbidding when these models arise, say, from a modified nodal analysis of integrated electronic circuits, or more broadly, from a spatial discretization of partial differential equations over a fine grid. Most dynamical systems arising in practice can be represented at least locally around an operating point, with a state-space representation having the form

$$\begin{aligned} E \dot{x} &= A x + B u, \\ y &= C x + D u, \end{aligned} \tag{1}$$

where $E \in \mathbb{R}^{N \times N}$ is the *descriptor matrix*, $A \in \mathbb{R}^{N \times N}$ is the system matrix and $x \in \mathbb{R}^N$, $u \in \mathbb{R}^m$, and $y \in \mathbb{R}^p$ ($p, m \ll N$) represent the state, input, and output of the system, respectively. A static feed-through relation from the control input u to the control output y is modeled through the matrix $D \in \mathbb{R}^{p \times m}$. Most practical systems involve several actuators (input variables) and several quantities of interest (output variables), motivating our focus here on systems having multiple inputs and multiple outputs (MIMO).

In many application settings, the state dimension N (which typically matches the order of the model) can grow quite large as greater model fidelity is pursued, and in some cases it can reach magnitudes of 10^6 and more. Simulation, optimization, and control design based on such large-scale models becomes computationally very expensive, at times even intractable. This motivates consideration of *reduced order models* (ROMs), which are comparatively low-order models that in spite of having significantly smaller order, $n \ll N$, are designed so as to reproduce the input-output response of the full-order model (FOM) accurately while preserving certain fundamental structural properties, that may include stability and passivity. For state space models such as (1), reduced models are obtained generally through Petrov-Galerkin projections having the form:

$$\begin{aligned} \overbrace{W^\top E V}^{E_r} \dot{x}_r &= \overbrace{W^\top A V}^{A_r} x_r + \overbrace{W^\top B}^{B_r} u, \\ y_r &= \underbrace{C V}_{C_r} x_r + D_r u. \end{aligned} \tag{2}$$

The projection matrices $V, W \in \mathbb{R}^{N \times n}$ become the primary objects of scrutiny in the model reduction enterprise, since how they are chosen has a great impact on the quality of the ROM. For truly large-scale systems, *interpolatory model reduction*, which includes approaches known variously as *moment matching* methods and *Krylov subspace* methods, has drawn signif-

icant interest due to its flexibility and comparatively low computational cost [2, 3, 4]. Indeed, these methods typically require only the solution of large (generally sparse) linear systems of equations, for which several optimized methods are available. Through the appropriate selection of V and W , it is possible to match the action of the transfer function

$$G(s) = C(sE - A)^{-1}B + D \quad (3)$$

along arbitrarily selected *input* and *output* tangent directions at arbitrarily selected (driving) frequencies. The capacity to do this is central to our approach and is stated briefly here as:

Theorem 1 ([5, 6]). *Let $G(s)$ be the transfer function matrix (3) of the FOM (1) and let $G_r(s)$ be the transfer function matrix of an associated ROM obtained through Petrov-Galerkin projection as in (2). Suppose $\sigma, \mu \in \mathbb{C}$ are complex scalars (“shifts”) that do not coincide with any eigenvalues of the matrix pencil (E, A) but otherwise are arbitrary. Let also $r \in \mathbb{C}^m$ and $l \in \mathbb{C}^p$ be arbitrary nontrivial tangent directions. Then*

$$G(\sigma) \cdot r = G_r(\sigma) \cdot r \quad \text{if } (A - \sigma E)^{-1} Br \in \text{Ran}(V), \quad (4a)$$

$$l^\top \cdot G(\mu) = l^\top \cdot G_r(\mu) \quad \text{if } (A - \mu E)^{-\top} C^\top l \in \text{Ran}(W), \quad (4b)$$

$$l^\top \cdot G'(\sigma) \cdot r = l^\top \cdot G'_r(\sigma) \cdot r \quad \text{if, additionally, } \sigma = \mu. \quad (4c)$$

A set of complex shifts, $\{\sigma_i\}_{i=1}^n$, $\{\mu_i\}_{i=1}^n$, with corresponding tangent directions, $\{r_i\}_{i=1}^n$, $\{l_i\}_{i=1}^n$, will be collectively referred to as *interpolation data* in our present context. We define *primitive projection matrices* as

$$\tilde{V} := [(A - \sigma_1 E)^{-1} B r_1, \dots, (A - \sigma_n E)^{-1} B r_n] \quad (5a)$$

$$\tilde{W} := [(A - \mu_1 E)^{-\top} C^\top l_1, \dots, (A - \mu_n E)^{-\top} C^\top l_n] \quad (5b)$$

Note that \tilde{V} and \tilde{W} satisfy Sylvester equations having the form:

$$A \tilde{V} - E \tilde{V} S_\sigma = B \tilde{R} \quad \text{and} \quad A^\top \tilde{W} - E^\top \tilde{W} S_\mu^\top = C^\top \tilde{L}, \quad (6)$$

where $S_\sigma = \text{diag}(\sigma_1, \dots, \sigma_n) \in \mathbb{C}^{n \times n}$, $S_\mu = \text{diag}(\mu_1, \dots, \mu_n) \in \mathbb{C}^{n \times n}$, $\tilde{R} = [r_1, \dots, r_n] \in \mathbb{C}^{m \times n}$ and $\tilde{L} = [l_1, \dots, l_n] \in \mathbb{C}^{p \times n}$ [7]. In this way, the Petrov-Galerkin projection of (2) is parameterized by interpolation data and the principal task in defining interpolatory models then becomes the judicious choice of shifts and tangent directions.

Procedures have been developed over the past decade for choosing interpolation data that yield reduced models, $G_r(s)$, that minimize, at least locally the approximation error, $G(s) - G_r(s)$, as measured with respect to the \mathcal{H}_2 -norm:

$$\|G - G_r\|_{\mathcal{H}_2} := \sqrt{\frac{1}{2\pi} \int_{-\infty}^{\infty} \|G(j\omega) - G_r(j\omega)\|_F^2 d\omega} \quad (7)$$

(see [2]). Minimizing the \mathcal{H}_2 -error, $\|G - G_r\|_{\mathcal{H}_2}$, is of interest through the immediate relationship this quantity bears with the induced system response error:

$$\|y - y_r\|_{\mathcal{L}_\infty} \leq \|G - G_r\|_{\mathcal{H}_2} \|u(t)\|_{\mathcal{L}_2}, \quad (8)$$

A well-known approach to accomplish this that has become popular at least in part due to its simplicity and effectiveness is the *Iterative Rational Krylov Algorithm* (IRKA) [8], which, in effect, runs a simple fixed point iteration aimed at producing interpolation data that satisfy first-order \mathcal{H}_2 -optimality conditions, i.e.,

$$G(-\lambda_i) \cdot \hat{b}_i = G_r(-\lambda_i) \cdot \hat{b}_i, \quad \hat{c}_i^\top \cdot G(-\lambda_i) = \hat{c}_i^\top \cdot G_r(-\lambda_i), \quad (9a)$$

$$\text{and } \hat{c}_i^\top \cdot G'(-\lambda_i) \cdot \hat{b}_i = \hat{c}_i^\top \cdot G_r'(-\lambda_i) \cdot \hat{b}_i. \quad (9b)$$

for $i = 1, \dots, n$. The data λ_i , \hat{b}_i and \hat{c}_i are reduced poles and right/left vector residues corresponding to the pole-residue expansion of the ROM:

$$G_r(s) = \sum_{i=1}^n \frac{\hat{c}_i \hat{b}_i^\top}{s - \lambda_i}. \quad (10)$$

Despite the relative ease with which \mathcal{H}_2 -optimal reduced models can be obtained, there are several circumstances in which it might be preferable to obtain a ROM which produces a small error as measured in the \mathcal{H}_∞ -norm:

$$\|G - G_r\|_{\mathcal{H}_\infty} := \max_{\omega} \varsigma_{max}(G(j\omega) - G_r(j\omega)), \quad (11)$$

where $\varsigma_{max}(M)$ denotes the largest singular value of a matrix M (see [2]). ROMs having small \mathcal{H}_∞ -error produce an output response with a uniformly bounded “energy” error:

$$\|y - y_r\|_{\mathcal{L}_2} \leq \|G - G_r\|_{\mathcal{H}_\infty} \|u\|_{\mathcal{L}_2}. \quad (12)$$

The \mathcal{H}_∞ -error is also used as a robustness measure for closed-loop control systems and is therefore of central importance in robust control. It finds frequent use in aerospace applications, among others, where the \mathcal{L}_2 energy of the system response is of critical interest in design and optimization.

Strategies for producing reduced models that give good \mathcal{H}_∞ performance has long been an active area of research [9]. Analogous to the \mathcal{H}_∞ -control design problem, the optimal \mathcal{H}_∞ reduction problem can be formulated in terms of *linear matrix inequalities*, although advantageous features such as linearity and convexity are lost in this case [10, 11]. Due to the high cost

related to solving these matrix inequalities, this approach is generally not feasible in large-scale settings.

Another family of methods for the \mathcal{H}_∞ reduction problem relates it to the problem of finding an *optimal Hankel norm approximation* (OHNA) [12, 13, 14]. Along these lines the *balanced truncation* (BT) algorithm yields rigorous upper bounds on the \mathcal{H}_∞ error and often produces small approximation error, especially for higher reduced order approximants [2, 15]. Each of these procedures is generally feasible only for mid-size problems since either an all-pass dilation requiring large-scale eigenvalue decomposition (for OHNA) or the solution of generalized Lyapunov equations (for BT) is required. Extensions to large-scale models are available, however – e.g., in [16, 17, 18, 19, 20, 21].

A wholly different approach to the \mathcal{H}_∞ model reduction problem for SISO models was proposed by Flagg, Beattie, and Gugercin in [1]. A locally \mathcal{H}_2 -optimal reduced model is taken as a starting point and adjusted through the variation of rank-one modifications parameterized by the scalar feed-through term, D . Minimization of the \mathcal{H}_∞ -error with respect to this parameterization available through D produces ROMs that are observed to have generally very good \mathcal{H}_∞ -performance, often exceeding what could be attained with OHNA.

In this work, we extend these earlier interpolatory methods to MIMO systems. We introduce a strategy that reduces the computational expense of the intermediate optimization steps by means of data-driven MOR methods (we use *vector fitting* [22, 23]). Stability of the reduced model is guaranteed through appropriate constraints in the resulting multivariate optimization problem. Numerical examples show effective reduction of approximation error, often outperforming both OHNA and BT.

2 MIMO Interpolatory \mathcal{H}_∞ -approximation (MIHA)

In this section we first characterize the \mathcal{H}_∞ -optimal reduced order models from the perspective of rational interpolation. This motivates the usage of \mathcal{H}_2 -optimal reduction as a starting point for the model reduction algorithm we propose for the \mathcal{H}_∞ approximation problem.

2.1 Characterization of \mathcal{H}_∞ -approximants via rational interpolation

In the SISO case, Trefethen [14] has characterized best \mathcal{H}_∞ approximations within a broader context of rational interpolation:

Theorem 2 (Trefethen [14]). *Suppose $G(s)$ is a (scalar-valued) transfer function associated with a SISO dynamical system as in (3). Let $\widehat{G}_r(s)$ be an optimal \mathcal{H}_∞ approximation to $G(s)$ and let G_r be any n^{th} order stable approximation to $G(s)$ that interpolates $G(s)$ at $2n + 1$ points in the open right half-plane. Then*

$$\min_{\omega \in \mathbb{R}} |G(j\omega) - G_r(j\omega)| \leq \|G - \widehat{G}_r\|_{\mathcal{H}_\infty} \leq \|G - G_r\|_{\mathcal{H}_\infty}$$

In particular, if $|G(j\omega) - G_r(j\omega)| = \text{const}$ for all $\omega \in \mathbb{R}$ then G_r is itself an optimal \mathcal{H}_∞ -approximation to $G(s)$.

For the SISO case, a good \mathcal{H}_∞ approximation will be obtained when the modulus of the error, $|G(s) - G_r(s)|$, is nearly constant as $s = j\omega$ runs along the imaginary axis. In the MIMO case, the analogous argument becomes more technically involved as the maximum singular value of matrix-valued function $G(s) - G_r(s)$ will not generally be analytic in the neighborhood of the imaginary axis (e.g., where multiple singular values occur). Nonetheless, the intuition of the SISO case carries over to the MIMO case, as the following *Gedankenexperiment* might suggest: Suppose that \widehat{G}_r is an \mathcal{H}_∞ -optimal interpolatory approximation to G but $\varsigma_{\max}(G(j\omega) - \widehat{G}_r(j\omega))$ is not constant with respect to $\omega \in \mathbb{R}$. Then there exist frequencies $\hat{\omega}$ and $\tilde{\omega} \in \mathbb{R}$ and $\epsilon > 0$ such that

$$\begin{aligned} \|G - \widehat{G}_r\|_{\mathcal{H}_\infty} = \varsigma_{\max}(G(j\hat{\omega}) - \widehat{G}_r(j\hat{\omega})) &\geq \epsilon + \min_{\omega} \varsigma_{\max}(G(j\omega) - \widehat{G}_r(j\omega)) \\ &= \epsilon + \varsigma_{\max}(G(j\tilde{\omega}) - \widehat{G}_r(j\tilde{\omega})). \end{aligned}$$

By nudging interpolation data away from the vicinity of $\tilde{\omega}$ and toward $\hat{\omega}$ while simultaneously nudging the poles of \widehat{G}_r away from the vicinity of $\hat{\omega}$ and toward $\tilde{\omega}$, one may decrease the value of $\varsigma_{\max}(G(j\hat{\omega}) - \widehat{G}_r(j\hat{\omega}))$ while increasing the value of $\varsigma_{\max}(G(j\tilde{\omega}) - \widehat{G}_r(j\tilde{\omega}))$. This will (incrementally) decrease the \mathcal{H}_∞ norm and bring the values of $\varsigma_{\max}(G(j\hat{\omega}) - \widehat{G}_r(j\hat{\omega}))$ and $\varsigma_{\max}(G(j\tilde{\omega}) - \widehat{G}_r(j\tilde{\omega}))$ closer together toward a common value.

Of course, the nudging process described above contains insufficient detail to suggest an algorithm, and indeed, our approach to this problem follows a somewhat different path, a path that nonetheless uses the guiding heuristic for (near) \mathcal{H}_∞ -optimality:

$$\varsigma_{\max}(G(j\omega) - \tilde{G}_r(j\omega)) \approx \text{const} \quad \text{for all } \omega \in \mathbb{R}. \quad (13)$$

Approximations with good \mathcal{H}_∞ performance should have an advantageous configuration of poles and interpolation data that locates them symmetrically about the imaginary axis, thus balancing regions where $\varsigma_{\max}(G(s) - \tilde{G}_r(s))$ is big (e.g., pole locations) symmetrically against regions reflected across the imaginary axis where $\varsigma_{\max}(G(s) - \tilde{G}_r(s))$ is small (e.g., interpolation locations). This configuration of poles and interpolation data, we note, is

precisely the outcome of optimal \mathcal{H}_2 approximation as well, and this will provide us with an easily computable approximation that is likely to have good \mathcal{H}_∞ performance.

2.2 \mathcal{H}_∞ approximation with interpolatory \mathcal{H}_2 -optimal initialization

Local \mathcal{H}_2 -optimal ROMs are often observed to give good \mathcal{H}_∞ performance – this is in addition to the expected good \mathcal{H}_2 performance. This \mathcal{H}_∞ behaviour is illustrated in Figure 1, where the \mathcal{H}_∞ approximation errors of local \mathcal{H}_2 -optimal ROMs produced by IRKA are compared to ROMs of the same order obtained through BT for the CD player MIMO benchmark model [24].

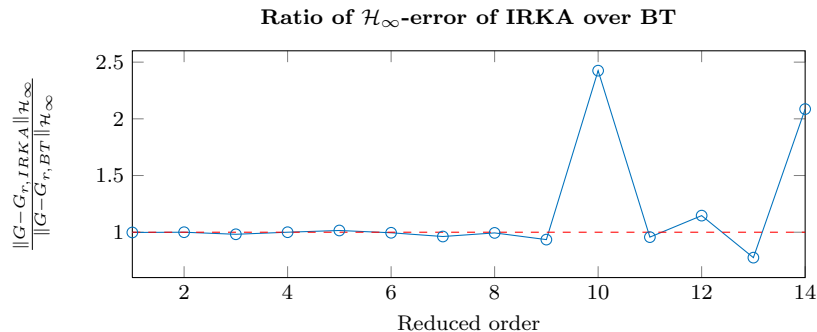


Fig. 1: Numerical investigations indicate that IRKA models are often good also in terms of the \mathcal{H}_∞ -error.

The frequently favourable \mathcal{H}_∞ behaviour of IRKA models has particular significance in this context, since they are computationally cheap to obtain even in large-scale settings, indeed often they are much cheaper than comparable BT computations. The resulting locally \mathcal{H}_2 -optimal ROMs can be further improved (with respect to \mathcal{H}_∞ error) by relaxing the (implicit) interpolation constraint at ∞ while preserving the \mathcal{H}_2 -optimal interpolation conditions (which is the most important link the \mathcal{H}_2 -optimal ROM has with the original model).

Consider the partial fraction expansion

$$G_r(s) = \sum_{i=1}^N \frac{\hat{c}_i \hat{b}_i^\top}{s - \lambda_i} + D_r. \quad (14)$$

For ease of exposition, we assume the poles, λ_i , to be simple, although the results we develop here can be extended to the case of higher multiplicity. The input/output behavior is determined by n scalar parameters λ_i , n pairs of input/output residuals \hat{b}_i, \hat{c}_i and the $p \times m$ -dimensional feed-through D_r . Considering that a constant scaling factor can be arbitrarily defined in the product of the residuals, this leaves us a total of $n(p+m) + p \cdot m$ parameters, $n(p+m)$ of which can be described in terms of two-sided tangential interpolation conditions (4). This interpolation data is established for the original \mathcal{H}_2 -optimal ROM and we wish it to remain invariant over subsequent adjustments, so the only remaining degrees-of-freedom are the $p \cdot m$ entries in the feed-through matrix D_r .

In the typical context of \mathcal{H}_2 -optimal model reduction, D_r is chosen to match the feed-through term D of the original model, thus guaranteeing that the error $G - \tilde{G}_r$ remains in \mathcal{H}_2 . Note that D remains untouched by the state-space projections in (2), moreover since typically $p, m \ll N$, the feed-through term need not be involved in the reduction process and may be retained from the FOM. Indeed, retaining the original feed-through term is a necessary condition for \mathcal{H}_2 optimality, forcing interpolation at $s = \infty$ and as a consequence, small error at higher frequencies. Contrasting significantly with \mathcal{H}_2 -based model reduction, good \mathcal{H}_∞ performance does not require $D_r = D$, and in this work we exploit this flexibility in a crucial way. A key observation playing a significant role in what follows was made in [25, 26] that the feed-through term D_r induces a parametrization of all reduced order models satisfying the two-sided tangential interpolation conditions.

This result is summarized by following theorem taken from [25, Thm. 4.1] and [26, Thm. 3]

Theorem 3. *Let \tilde{R}, \tilde{L} be defined through the Sylvester equations in (6). Assume, without loss of generality, that the full order model satisfies $D = 0$ and let the nominal reduced model $G_r^0(s) = C_r (sE_r - A_r)^{-1} B_r$ be obtained through Petrov-Galerkin projection using the primitive projection matrices (5). Then, for any $D_r \in \mathbb{C}^{p \times m}$, the perturbed reduced order model*

$$\tilde{G}_r^D(s, D_r) = \left(\tilde{C}_r + D_r \tilde{R} \right) \left[s \tilde{E}_r - \left(\tilde{A}_r + \tilde{L}^\top D_r \tilde{R} \right) \right]^{-1} \left(\tilde{B}_r + \tilde{L}^\top D_r \right) + D_r \quad (15)$$

also satisfies the tangential interpolation conditions (4).

Note that for $D \neq 0$, the results of Theorem 3 can be trivially extended by adding D to the right-hand side in (15). Even though for theoretical consideration the use of primitive Krylov bases \tilde{V}, \tilde{W} introduced in (5) is often convenient, from a numerical standpoint there are several reasons why one may choose a different basis for the projection matrices. This next result shows that the interpolation conditions are preserved also for arbitrary bases—in particular also real and orthonormal bases—provided that the shifting matrices R and L are appropriately chosen.

Corollary 1. Let $T_v, T_w \in \mathbb{C}^{n \times n}$ be invertible matrices used to transform the primitive bases \tilde{V}, \tilde{W} of the Krylov subspace to new bases $V = \tilde{V}T_v$ and $W = \tilde{W}T_w$. Let the same transformation be applied to the matrices of tangential directions, resulting in $R = \tilde{R}T_v$ and $L = \tilde{L}T_w$. Then, for any D_r , the ROM G_r^D is given by

$$G_r^D(s, D_r) = \underbrace{(C_r + D_r R)}_{C_r^D} \left[sE_r - \underbrace{(A_r + L^\top D_r R)}_{A_r^D} \right]^{-1} \underbrace{(B_r + L^\top D_r)}_{B_r^D} + D_r \quad (16)$$

Proof. The proof amounts to showing that the transfer function matrix G_r^D of the ROM is invariant to a change of basis from \tilde{V} and \tilde{W} as long as \tilde{R} and \tilde{L} are adapted accordingly.

$$\begin{aligned} G_r^D - D_r &= C_r^D (sE - A_r^D)^{-1} B_r^D \\ &= (CV + D_r R) [sW^\top EV - W^\top AV - L^\top D_r R^\top]^{-1} (W^\top B + L^\top D_r) \\ &= (C\tilde{V} + D_r \tilde{R}) T_v \left[T_w^\top (s\tilde{W}^\top E\tilde{V} - \tilde{W}^\top A\tilde{V} - \tilde{L}^\top D_r \tilde{R}^\top) T_v \right]^{-1} T_w^\top (\tilde{W}^\top B + \tilde{L}^\top D_r) \\ &= (C\tilde{V} + D_r \tilde{R}) [s\tilde{W}^\top E\tilde{V} - \tilde{W}^\top A\tilde{V} - \tilde{L}^\top D_r \tilde{R}^\top]^{-1} (\tilde{W}^\top B + \tilde{L}^\top D_r) \\ &= \tilde{G}_r^D - D_r. \end{aligned}$$

The results of Theorem 3 generalize to the case of arbitrary bases. Following the notation from [25, Definition 2.1], the state-space models resulting from Petrov-Galerkin projections with V, W and \tilde{V}, \tilde{W} respectively are *restricted system equivalent*. As a consequence, they share the same transfer function matrix.

Using the Sherman-Morrison-Woodbury formula [27] for the inverse of rank k perturbations of a matrix, we are able to decompose the transfer function of the shifted reduced model into the original reduced model and an additional term.

Corollary 2. Define the auxiliary variable $\mathcal{K}_r := sE_r - A_r$. The transfer function of the shifted reduced model G_r^D can be given as

$$G_r^D(s) = G_r^0(s) + \Delta G_r^D(s, D_r), \quad (17)$$

where G_r^0 is the transfer function of the unperturbed model and ΔG_r^D is defined as

$$\begin{aligned} \Delta G_r^D &= \Delta_1 + \Delta_2 + \Delta_3 \cdot (\Delta_4)^{-1} \cdot \Delta_2 + D_r \\ &\text{given} \\ \Delta_1 &:= C_r \mathcal{K}_r^{-1} L^\top D_r & \Delta_2 &:= D_r R \mathcal{K}_r^{-1} (B_r + L^\top D_r) \\ \Delta_3 &:= (C_r + D_r R) \mathcal{K}_r^{-1} L^\top & \Delta_4 &:= I - D_r R \mathcal{K}_r^{-1} L^\top \end{aligned} \quad (18)$$

Proof. Note that by the Sherman-Morrison-Woodbury formula, following equality holds:

$$(\mathcal{K}_r - L^\top D_r R)^{-1} = \mathcal{K}_r^{-1} + \mathcal{K}_r^{-1} L^\top (I - D_r R \mathcal{K}_r^{-1} L^\top)^{-1} D_r R \mathcal{K}_r^{-1}. \quad (19)$$

Using this relation in the definition of G_r^D , the proof is completed by straightforward algebraic manipulations.

We proceed by attempting to exploit the additional degrees-of-freedom available in D_r to trade off excessive accuracy at high frequencies for improved approximation in lower frequency ranges, as measured with the \mathcal{H}_∞ -norm. We first obtain an \mathcal{H}_2 -optimal ROM by means of IRKA and subsequently minimize the \mathcal{H}_∞ -error norm with respect to the constant feed-through matrix D_r while preserving tangential interpolation and guaranteeing stability. The resulting ROM G_r^* will represent a local optimum out of the set of all stable ROMs satisfying the tangential interpolation conditions. The outline of our proposed reduction procedure, called *MIMO interpolatory \mathcal{H}_∞ -approximation* (MIHA), is given in Algorithm 1.

Algorithm 1 MIMO Interpolatory \mathcal{H}_∞ -Approximation (MIHA)

Input: $G(s)$, n

Output: Stable, locally optimal reduced order model G_r^* , approximation error $e_{\mathcal{H}_\infty}^*$

1: $G_r^0 \leftarrow \text{IRKA}(G(s), n)$

2: $D_r^* \leftarrow \arg \min_{D_r} \|G(s) - G_r^D(s, D_r)\|_{\mathcal{H}_\infty}$ s.t. $G_r^D(s, D_r^*)$ is stable

3: $G_r^* \leftarrow G_r^D(s, D_r^*)$

4: $e_{\mathcal{H}_\infty}^* \leftarrow \|G(s) - G_r^*(s)\|_{\mathcal{H}_\infty}$

Numerical results in Section 3 will show the effectiveness of this procedure in further reducing the \mathcal{H}_∞ -error for a given IRKA model. However, at this stage the optimization in Step 2 appears problematic, for it requires both the computation of the \mathcal{H}_∞ -norm of a large-scale model and a constrained multivariate optimization of a non-convex, non-smooth function. It turns out that both of these issues can be resolved effectively, as it will be discussed in the following sections.

2.3 Efficient implementation

As we have noted, the main computational burden of the algorithm described above resides mainly in Step 2. We are able to lighten this burden somewhat through judicious use of (17) and by taking advantage of previously computed transfer function evaluations.

2.3.1 A “free” surrogate model for the approximation error $G - G_r^0$

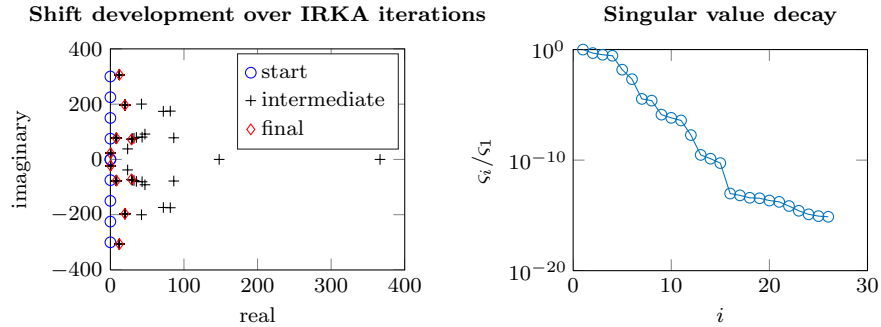
Step 1 of Algorithm 1 requires performing \mathcal{H}_2 -optimal reduction using IRKA. This is a fixed point iteration involving a number of steps k before convergence is achieved. At every step j , Hermite tangential interpolation about some complex frequencies $\{\sigma_i\}_{i=1}^n$ and tangential directions $\{r_i\}_{i=1}^n, \{l_i\}_{i=1}^n$ is performed. For this purpose, the projection matrices in (5) are computed, and it is easy to see that for all $i = 1, \dots, n$ it holds

$$C \cdot \tilde{V} e_i = C (A - \sigma_i E)^{-1} B r_i = G(\sigma_i) r_i \quad (20a)$$

$$e_i^\top \tilde{W}^\top \cdot B = l_i^\top C (A - \sigma_i E)^{-1} B = l_i^\top G(\sigma_i) \quad (20b)$$

$$e_i^\top \tilde{W}^\top E \tilde{V} e_i = l_i^\top (A - \sigma_i E)^{-1} E (A - \sigma_i E)^{-1} r_i = l_i^\top G'(\sigma_i) r_i \quad (20c)$$

Observe that, at basically no additional cost, we can gather information about the FOM while performing IRKA. Figure 2a illustrates this point by showing the development of the shifts during the IRKA iterations reducing the CDplayer benchmark model to a reduced order $n = 10$. For all complex frequencies indicated by a marker, tangent data for the full order model is collected.



(a) Points at which data of the FOM is collected during IRKA.

(b) Decay of singular values of the matrix $[\mathbb{L}, \sigma \mathbb{L}]$ for the data collected during IRKA.

Fig. 2: Data collecting during IRKA can be used to generate data-driven surrogates.

To use this “free” data, there are various choices for “data-driven” procedures that produce useful rational approximations. *Loewner methods* [25, 28, 29, 30] are effective and are already integrated into IRKA iteration strategies [31]. We adopt here a *vector fitting* strategy [22, 32, 33, 23, 34] instead. This allows us to produce stable low-order approximations of the reduction error after IRKA

$$\widetilde{G}_e^0 \approx G_e^0 := G - G_r^0. \quad (21)$$

An appropriate choice of order for the surrogate model can be obtained by forming the Loewner \mathbb{L} and shifted Loewner $\sigma\mathbb{L}$ matrices from G and G' evaluations that were generated in the course of the IRKA iteration and then observing the singular value decay of the matrix $[\mathbb{L}, \sigma\mathbb{L}]$, as indicated in Figure 2b.

Using the decomposition in (17), the \mathcal{H}_∞ -norm evaluations required during the optimization will be feasible even for large-scale full order models. In addition, it will allow us to obtain a cheap estimate $\tilde{e}_{\mathcal{H}_\infty}$ for the approximation error

$$e_{\mathcal{H}_\infty} := \|G - G_r^D\|_{\mathcal{H}_\infty} \approx \left\| \widetilde{G}_e^0 - \Delta G_r^D \right\|_{\mathcal{H}_\infty} = \tilde{e}_{\mathcal{H}_\infty} \quad (22)$$

2.3.2 Constrained multivariate optimization with respect to D_r

The focus of this work lies in the development of new model reduction strategies. Our intent is not directed toward making a contribution to either the theory or practice of numerical optimization and we are content in this work to use standard optimization approaches. In the results of section 3, we rely on state-of-the-art algorithms that are widespread and available, e.g., in MATLAB. With that caveat understood, we do note that the constrained multivariate optimization over the reduced feed-through, D_r , is a challenging optimization problem, so we will explain briefly the setting that seems to work best in our case. The computation and optimization of \mathcal{H}_∞ -norms for large-scale models remains an active area of research, as demonstrated by [35, 36, 37].

The problem we need to solve in step 2 of Algorithm 1 is

$$\begin{aligned} \min_{D_r \in \mathbb{R}^{p \times m}} \quad & \max_{\omega} \varsigma_{max} (G(j\omega) - G_r^D(j\omega, D_r)) \\ \text{s.t.} \quad & G_r^D(s, D_r) \text{ is stable} \end{aligned} \quad (23)$$

which represents a non-smooth, non-convex multivariate optimization problem in a $p \times m$ -dimensional search space. In our experience, the best strategy considering both optimization time and optimal solution is given by a combination of *coordinate descent* (CD) [38] and subsequent *multivariate optimization* (MV). We refer to this combined strategy as CV+MV. The coordinate descent strategy is used in this setting somewhat like an initialization procedure to find a better starting point than $D_r^0 = 0$. This initialization is based on reducing the search space from $p \cdot m$ dimensions to just one, hence performing a much simpler univariate optimization in each step. Once one cycle has been conducted for all elements in the feed-through matrix, the resulting feed-through is used to initialize a nonlinear constrained optimization solver that minimizes the error with respect to the whole D_r matrix. We have used a sequential quadratic programming (SQP) method as implemented in

MATLAB's `fmincon`, although acceptable options for this final step abound. Further information about optimization strategies can be found in [39].

The suitability of CD+MV is motivated by extensive simulations conducted comparing different strategies, such as direct multivariate optimization, *global search* (GS) [40], and *genetic algorithms* (GA) (cp. Figure 3). Ultimately, we rely on the results of Section 3 to show that this procedure is effective.

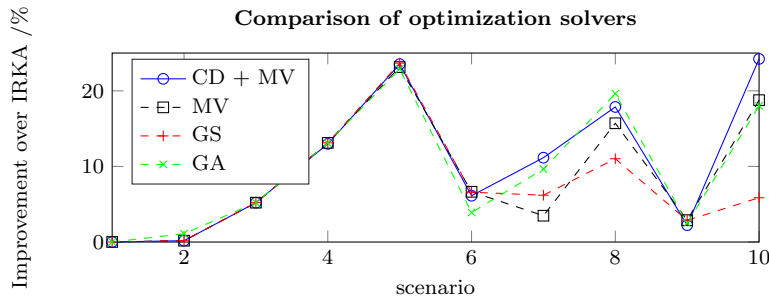


Fig. 3: Comparison of different solvers shows the effectiveness of coordinate descent followed by multivariate optimization.

3 Numerical results

In the following we demonstrate the effectiveness of the proposed procedure by showing reduction results with different MIMO models. The reduction code is based on the `sssMOR` toolbox² [41]. For generation of vector fitting surrogates, we use the `vectfit3` function³ [22, 32, 33]. Note that more recent implementation of MIMO vector fitting introduced in [23] could be used instead, especially for improved robustness.

3.1 Heat model

Our proposed procedure is demonstrated through numerical examples conducted on a MIMO benchmark model representing a discretized heat equation of order $N = 197$ with $p = 2$ outputs and $m = 2$ inputs [42].

² Available at www.rt.mw.tum.de/?sssMOR.

³ Available at www.sintef.no/projectweb/vectfit/downloads/vfut3/.

Model reduction for this model was conducted for a range of reduced orders; the results are summarized in Table 1. The table shows the reduced order n , the order n_m of the error surrogate \widehat{G}_e^0 , and the relative \mathcal{H}_∞ error of the proposed ROM G_r^D , as well as the percentage improvement over the initial IRKA model. Our proposed method improves significantly on the \mathcal{H}_∞ performance of IRKA, in some cases by more than 50%.

Table 1: Results for the heat model problem

n	1	2	3	4	5	6	7	8	9	10
n_m	14	24	20	22	24	30	32	36	36	36
$\frac{\ G - G_r^D\ }{\ G\ }$	8.7e-02	7.6e-03	1.2e-02	1.2e-03	6.5e-04	5.7e-04	4.1e-04	1.6e-04	4.4e-05	8.6e-06
$1 - \frac{\ G - G_r^D\ }{\ G - G_r^0\ }$	50.8%	39.0%	27.0%	36.7%	36.0%	44.8%	52.0%	44.6%	49.5%	42.6%

Figure 4 gives a graphical representation of the reduction results. The plots compare the approximation error achieved after applying MIHA, with a vector fitting surrogate as described in Section 2.3.1, to other reduction strategies. These include the direct reduction with IRKA, balanced truncation (BT), Optimal Hankel Norm Approximation (OHNA) as well as the optimization with respect to the actual error G_e^0 (MIHA without surrogate). For a better graphical comparison throughout the reduced orders studied, the errors are related to the theoretical lower bound given by

$$\underline{e}_{\mathcal{H}_\infty} := \varsigma_{n+1}^H, \quad (24)$$

with which we denote the Hankel singular value of order $n + 1$.

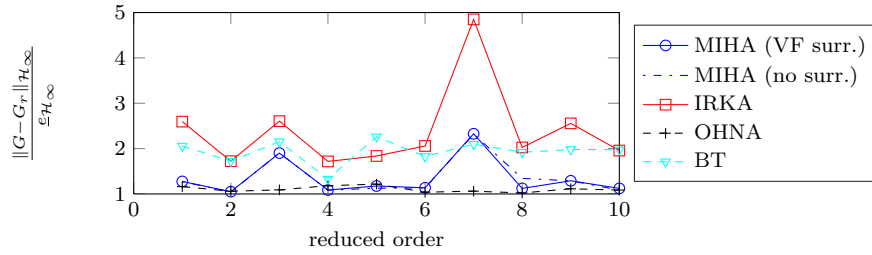


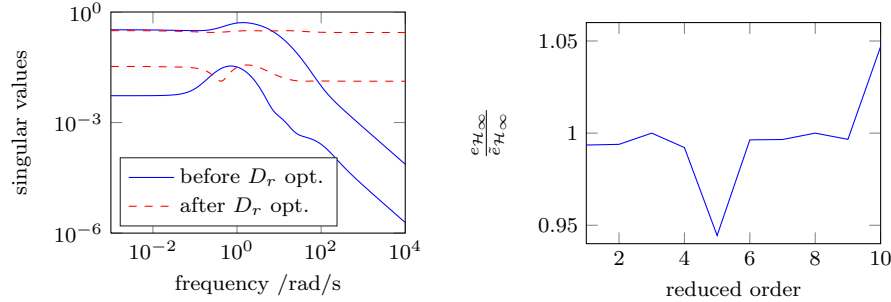
Fig. 4: Plot of the approximation error relative to the theoretical error bound.

Notice how effectively the ROMs resulting from the D_r -optimization reduce the \mathcal{H}_∞ -error beyond what is produced by the IRKA ROMs and that they often, (here, in 9 out of 10 cases) yield better results than BT and sometimes (here, in 3 out of 10 cases) yield better results even than OHNA.

Note also that the optimization with respect to the vector-fitting surrogate produces as good a result as optimization with respect to the true error. For reduced order $n = 8$, optimization with respect to the surrogate yields even a better result. This is not expected and may be due to the different cost functions involved, causing optimization of the true error to converge to a worse solution.

The plot also confirms our initial motivation in using IRKA models as starting points, since their approximation in terms of the \mathcal{H}_∞ norm is often not far from BT. Finally, note how in several cases the resulting ROM is very close to the theoretical lower bound, which implies that the respective ROMs are not far from being the *global* optimum.

Figure 5a shows the approximation error before and after the feed-through optimization for a selected reduced order of 2. The largest singular value is drastically reduced (ca. 40%) by lifting up the value at high frequencies. This confirms our intuition that the \mathcal{H}_∞ -optimal reduced order model should have a nearly constant error modulus over all frequencies. Finally, Figure 5b demonstrates the validity of the error estimate $\tilde{e}_{\mathcal{H}_\infty}$ obtained using the surrogate model.



(a) Singular value plot of the error before and after optimization.

(b) Comparison of error estimate $\tilde{e}_{\mathcal{H}_\infty}$ versus true error $e_{\mathcal{H}_\infty}$.

Fig. 5: Optimization with the surrogate effectively reduces and provides an accurate estimate of the true error.

3.2 ISS model

Similar simulations were conducted on a MIMO model with $m = 3$ inputs and $p = 3$ outputs of order $N = 270$, representing the 1r component of the International Space Station (ISS) [24]. The results are summarized in Table 2 and Figure 6. Note that the \mathcal{H}_∞ -error after IRKA is comparable to that

Table 2: Results for the ISS problem

n	2	4	6	8	10	12	14	16	18	20
n_m	12	18	12	18	18	15	42	48	30	30
$\frac{\ G-G_r^D\ }{\ G\ }$	2.7e-01	9.4e-02	8.4e-02	7.9e-02	3.6e-02	3.4e-02	2.2e-02	2.2e-02	1.0e-02	7.7e-03
$1 - \frac{\ G-G_r^D\ }{\ G-G_r^0\ }$	7.5 %	9.9%	8.8%	4.9%	9.5%	13.8%	23.3%	15.7%	3.5%	25.8%

of BT and the proposed procedure is effective in further reducing the error, outperforming BT in all cases investigated. Finally, note also in this case

Error norms with respect to the theoretical lower bound

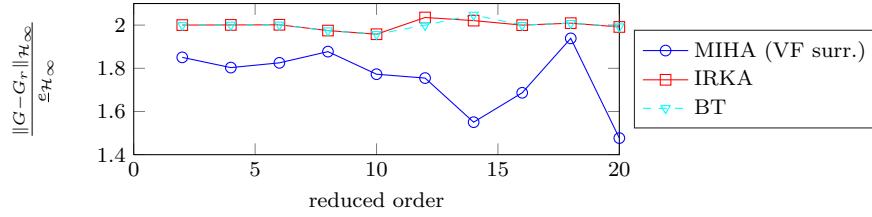


Fig. 6: Plot of the approximation error relative to the theoretical error bound (ISS).

that the modulus of the error due to this \mathcal{H}_∞ -approximation procedure is nearly constant, as anticipated. This is demonstrated in Figure 7, where the error plots for the reduction order $n = 10$ are compared.

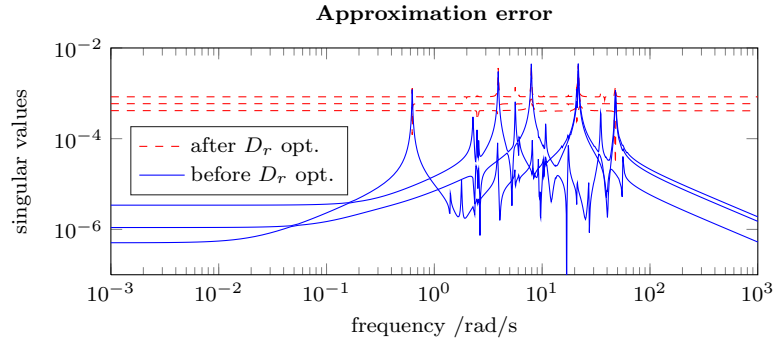


Fig. 7: Singular value plot of the error before and after optimization (ISS).

References

1. Garret M Flagg, C. A. Beattie, and Serkan Gugercin. Interpolatory \mathcal{H}_∞ model reduction. *Systems & Control Letters*, 62(7):567–574, 2013.
2. A. C. Antoulas. *Approximation of Large-Scale Dynamical Systems*. SIAM, 2005.
3. Kyle A. Gallivan, Antoine Vandendorpe, and Paul Van Dooren. On the generality of multipoint padé approximations. In *15th IFAC World Congress on Automatic Control*, 2002.
4. C. A. Beattie and Serkan Gugercin. Model reduction by rational interpolation. Accepted to appear in *Model Reduction and Approximation for Complex Systems*, 2014.
5. Eric J. Grimme. *Krylov Projection Methods for Model Reduction*. PhD thesis, Dep. of Electrical Eng., Uni. Illinois at Urbana Champaign, 1997.
6. Kyle A. Gallivan, A Vandendorpe, and Paul Van Dooren. Model reduction of mimo systems via tangential interpolation. *SIAM Journal on Matrix Analysis and Applications*, 26(2):328–349, 2004.
7. Kyle A. Gallivan, Antoine Vandendorpe, and Paul Van Dooren. Sylvester equations and projection-based model reduction. *Journal of Computational and Applied Mathematics*, 162(1):213–229, 2004.
8. Serkan Gugercin, A. C. Antoulas, and C. A. Beattie. \mathcal{H}_2 model reduction for large-scale linear dynamical systems. *SIAM Journal on Matrix Analysis and Applications*, 30(2):609–638, 2008.
9. AC Antoulas and A Astolfi. \mathcal{H}_∞ -norm approximation. *Unsolved problems in Mathematical Systems and Control Theory*, V. Blondel and A. Megretski Editors, pages 267–270, 2002.
10. Anders Helmerson. Model reduction using lmis. 1994.
11. Andras Varga and Pablo Parrilo. Fast algorithms for solving hinf-norm minimization problems. In *Decision and Control, 2001. Proceedings of the 40th IEEE Conference on*, volume 1, pages 261–266. IEEE, 2001.
12. Davut Kavranoglu and Maamar Bettayeb. Characterization of the solution to the optimal hinf model reduction problem. *Systems & Control Letters*, 20(2):99–107, 1993.
13. Keith Glover. All optimal hankel-norm approximations of linear multivariable systems and their linf-error bounds. *International journal of control*, 39(6):1115–1193, 1984.
14. L.N. Trefethen. Rational Chebyshev approximation on the unit disk. *Numerische Mathematik*, 37(2):297–320, 1981.
15. Serkan Gugercin and Athanasios C Antoulas. A survey of model reduction by balanced truncation and some new results. *International Journal of Control*, 77(8):748–766, 2004.
16. Peter Benner, Enrique S Quintana-Ortí, and Gregorio Quintana-Ortí. Computing optimal hankel norm approximations of large-scale systems. In *Decision and Control, 2004. CDC. 43rd IEEE Conference on*, volume 3, pages 3078–3083. IEEE, 2004.
17. Jing-Rebecca Li. *Model reduction of large linear systems via low rank system gramians*. PhD thesis, Massachusetts Institute of Technology, 2000.
18. Peter Benner, Patrick Kürschner, and Jens Saak. Self-generating and efficient shift parameters in ADI methods for large Lyapunov and Sylvester equations. *Electronic Transactions on Numerical Analysis*, 43:142–162, 2014.
19. Patrick Kürschner. *Efficient Low-Rank Solution of Large-Scale Matrix Equations*. PhD thesis, Otto-von-Guericke Universität Magdeburg, 2016.
20. John Sabino. *Solution of large-scale Lyapunov equations via the block modified Smith method*. PhD thesis, Citeseer, 2006.
21. Serkan Gugercin, Danny C Sorensen, and Athanasios C Antoulas. A modified low-rank smith method for large-scale Lyapunov equations. *Numerical Algorithms*, 32(1):27–55, 2003.

22. Bjørn Gustavsen and Adam Semlyen. Rational approximation of frequency domain responses by vector fitting. *Power Delivery, IEEE Transactions on*, 14(3):1052–1061, 1999.
23. Z. Drmač, S. Gugercin, and C. Beattie. Vector fitting for matrix-valued rational approximation. *SIAM Journal on Scientific Computing*, 37(5):A2346–A2379, 2015.
24. Younes Chahlaoui and Paul Van Dooren. A collection of benchmark examples for model reduction of linear time invariant dynamical systems. Working Note 2002-2, 02 2002.
25. A.J. Mayo and A. C. Antoulas. A framework for the solution of the generalized realization problem. *Linear Algebra and Its Applications*, 425(2–3):634–662, 2007.
26. C. A. Beattie and Serkan Gugercin. Interpolatory projection methods for structure-preserving model reduction. *Systems & Control Letters*, 58-3:225–232, 2009.
27. Gene H Golub and Charles F Van Loan. *Matrix computations*, volume 3. JHU Press, 2012.
28. AC Antoulas and BDQ Anderson. On the scalar rational interpolation problem. *IMA Journal of Mathematical Control and Information*, 3(2-3):61–88, 1986.
29. BDO Anderson and AC Antoulas. Rational interpolation and state-variable realizations. *Linear Algebra and its Applications*, 137:479–509, 1990.
30. Sanda Leteriu and Athanasios C Antoulas. A new approach to modeling multiport systems from frequency-domain data. *Computer-Aided Design of Integrated Circuits and Systems, IEEE Transactions on*, 29(1):14–27, 2010.
31. C. A. Beattie and Serkan Gugercin. Realization-independent \mathcal{H}_2 -approximation. In *51st IEEE Conference on Decision and Control*, pages 4953–4958. IEEE, 2012.
32. Bjorn Gustavsen. Improving the pole relocating properties of vector fitting. *Power Delivery, IEEE Transactions on*, 21(3):1587–1592, 2006.
33. Dirk Deschrijver, Michal Mrozowski, Tom Dhaene, and Daniel De Zutter. Macromodeling of multiport systems using a fast implementation of the vector fitting method. *Microwave and Wireless Components Letters, IEEE*, 18(6):383–385, 2008.
34. Z Drmac, S Gugercin, and C Beattie. Quadrature-based vector fitting for discretized h₂ approximation. *SIAM Journal on Scientific Computing*, 37(2):A625–A652, 2015.
35. Tim Mitchell and Michael L Overton. Fixed low-order controller design and \mathcal{H}_∞ optimization for large-scale dynamical systems. *IFAC-PapersOnLine*, 48(14):25–30, 2015.
36. Tim Mitchell and Michael L Overton. Hybrid expansion–contraction: a robust scaleable method for approximating the \mathcal{H}_∞ norm. *IMA Journal of Numerical Analysis*, page drv046, 2015.
37. N. Aliyev, P. Benner, E. Mengi, and M. Voigt. Large-scale computation of \mathcal{H}_∞ norms by a greedy subspace method. *Submitted to SIAM J. Matrix Anal. Appl.*, 2016.
38. Stephen J Wright. Coordinate descent algorithms. *Mathematical Programming*, 151(1):3–34, 2015.
39. Jorge Nocedal and Stephen Wright. *Numerical optimization*. Springer Science & Business Media, 2006.
40. Zsolt Ugray, Leon Lasdon, John Plummer, Fred Glover, James Kelly, and Rafael Mart. Scatter search and local nlp solvers: A multistart framework for global optimization. *INFORMS Journal on Computing*, 19(3):328–340, 2007.
41. Alessandro Castagnotto, Maria Cruz Varona, Lisa Jeschek, and Boris Lohmann. sss & sssMOR: Analysis & reduction of large-scale dynamic systems with MATLAB. In Preparation.
42. A. C. Antoulas, D. C. Sorensen, and S. Gugercin. A survey of model reduction methods for large-scale systems. *Structured Matrices in OperaStructured, Numerical Analysis, Control, Signal and Image Processing, Contemporary Mathematics, AMS publications*, 280:193–219, 2001.